Synchronized Electromechanical Shock Wave-Induced Bacterial Transformation

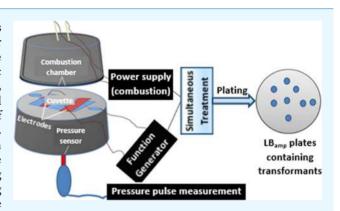Rishi Kant,[†,∥] Geeta Bhatt,[†,∥] Vinay Kumar Patel,[†,∥] Anurup Ganguli,[†] Deepak Singh,[‡] Monalisha Nayak,[†] Keerti Mishra,[‡] Ankur Gupta,[†] Keshab Gangopadhyay,[§] Shubhra Gangopadhyay,[§] Gurunath Ramanathan,[‡] and Shantanu Bhattacharya*,[†]

[†]Microsystems Fabrication Laboratory, Department of Mechanical Engineering and [‡]Department of Chemistry, Indian Institute of Technology Kanpur, Kanpur 208016, Uttar Pradesh, India

[§]Department of Electrical and Computer Engineering, University of Missouri Columbia, Columbia, Missouri 65211, United States

S *Supporting Information*

ABSTRACT: We report a simple device that generates synchronized mechanical and electrical pressure waves for carrying out bacterial transformation. The mechanical pressure waves are produced by igniting a confined nanoenergetic composite material that provides ultrahigh pressure. Further, this device has an arrangement through which a synchronized electric field (of a time-varying nature) is initiated at a delay of ≈85 μs at the full width half-maxima point of the pressure pulse. The pressure waves so generated are incident to a thin aluminum−polydimethylsiloxane membrane that partitions the ignition chamber from the column of the mixture containing bacterial cells (*Escherichia coli* BL21) and 4 kb transforming DNA. A combination of mechanical and electrical pressure pulse created through the above arrangement ensures that the transforming DNA transports across the cell membrane into the cell, leading to a transformation event. This unique device has been successfully operated for efficient gene (∼4 kb) transfer into cells. The transformation efficacy of this device is found comparable to the other standard methods and protocols for carrying out the transformation.

INTRODUCTION

Bacterial transformation is a powerful tool in genetic engineering and is of great importance in molecular cloning and environmental microbiology.[1] It is widely used in high-throughput studies, such as developing random gene libraries.[2] Transfer of DNA into bacterial cells takes place through some natural methods like transformation, transduction, and conjugation.[3] All of these methods are not promising due to restrictions like a limited host range of bacteriophage and the requirement of physical contact between the recipient and the donor with the involvement of a third bacteria containing the helper plasmid.[4,5] The increased search for improved methods to efficiently deliver molecular and genetic materials into cells has been a core interest area for the engineering community pursuing the advancement of gene therapy techniques.[6] The current procedures for molecular transport into cells are broadly classified into two basic categories: viral and nonviral.[7,8] The viral carriers such as adenoviruses and retroviruses show high delivery efficiency but lack in target specificity and maximum allowable therapeutic gene size.[7,8] The nonviral carriers, such as electroporation,[9] sonoporation,[10] gene-gun,[11] chemical carrier delivery,[12] microinjection,[13] ultrasound,[14] laser irradiation,[15] and mineral nanofibres,[16]

although less toxic than their viral counterparts, are limited in their efficiency, lack target specificity, and possess high cell mortality.

With the rapid emergence of the DNA recombinant technology and the fast evolution of bacterial genome sequencing, there is an increased demand for developing an easier, quicker, and effective transformation technique. Among nonviral transformation methods, the use of pressure waves for inducing temporary cell permeabilization for facilitating foreign molecule transport has been identified as a promising technique.[17] The nonviral vector transformation methods, such as electrotransfer or pressure wave transportation, create nonspecific and transient membrane permeability, and the molecular transport finally occurs through these artificially created pores on the membrane surface. Pressure waves with wave speeds traveling at 1.5 Mach for gene delivery applications can be generated by methods like shock wave lithotripsy,[18] shock tube,[19] and laser ablation[20] and by the burning of nanoenergetic composites that are capable of quick

Table 1. Effect of a Varying Electric Field Coupled with Mechanically Pressurized Pulse

	number of transformants at different voltages				
nanoenergetic material (mg)	0 V	2.5 V	5 V	7.5 V	10 V
25	29 ± 5	142 ± 4	291 ± 7	149 ± 6	125 ± 5

energy release.[21] Gangopadhyay et al.[21] reported delivery of fluorescein isothiocyanate-dextran in chicken heart cells using pressure waves generated from the combustion of nano-thermite materials. Prakash et al.[22] reported the transformation of *Escherichia coli* DH5α cells with green fluorescent protein (GFP) plasmids (size ~5.37 kb) through shockwaves using explosive-coated polymer tubes to achieve higher trans-formation efficiency.

The other primary nonviral vector transformation methods like electrotransformation method was developed long back in 1980 where ultrahigh external electric field pulses (of the order of ~6.25 kV/cm) were deployed to cause cell membrane permeabilization followed by the electrophoretic transport of negatively charged DNA across the permeabilized cells.[23−25] Due to the Joule heating effects,[26] the method although having good yield had severe limitations of high cell mortality and subsequent cell lysis. The electrotransfer process has been well characterized as a multistep process with electropermeabiliza-tion of the cell membrane, anchoring of the plasmid to the permeabilized cell membrane, and finally the diffusive transport of such plasmid into the intercellular cytoplasm.[27,28] Further, the electrophoretic component of DNA electro-transfer has been found to have a significant impact on the overall transformation efficiency.[29,30] For example, the use of high-voltage (for membrane permeabilization) and low-voltage (for electrotransfer) pulses in combination has been found to produce greater yield than that found using a single high-voltage pulse.[31]

Further, in some enterobacterial species, such as *Salmonella typhimurium*[32] and *Pseudomonas aeruginosa*,[33] the chemical methods of gene transfer are altogether ineffective in comparison with some other species like *E. coli*. For such strains, nonviral vector transformation method of electro-poration has been observed to be an appropriate alternative that also enriches the vitality of the nonviral transport process. This electroporation technique also serves as a potent tool to perform gene transfer in mammalian cells that have further complexity in terms of transforming DNA across cellular and subsequently another nuclear membrane.[34,35] The transient permeabilization of the plasma membrane under the influence of an external electric field increases drastically by the electroporation technique.[36] The majority of electroporation techniques are mainly based on the application of short voltage pulses, the precision of which is enhanced through the designs of microfluidic platforms.[37−42] In the majority of such electroporation setups, there is increased use of direct current (DC) sources. Very few reports indicate the use of alternative current fields for performing transformation.[43−45] The essential design requirement to realize a suitable transformation method is one that can achieve high targeted yield and overall low cell mortality. From the above analysis, it is observed that although the pressure-mediated transformation may have lesser cell mortality, it has lower targeted yield.

On the other hand, the electroporation process has a high yield although it is severely limited by lower viability of transformants. So, a good method design would need the combination of the best part of each pressure-mediated and electroporation methods. Also, short pulse DC signals have shown good yields earlier in terms of targeted delivery of the transforming DNA.

In this work, we have explored a hybrid platform that couples intense mechanical pressure pulses augmented by synchronous electrical pulses to carry out transformation. The electric pulses are generated in a time-controlled manner through the circuit, as shown in the Supporting Information (Figure S1), and have a role of electrotransfer of transforming DNA apart from augmenting the overall pressure level. The root mean square voltage magnitude being quite low does not cause a significant rise in the Joule temperature and results in targeted delivery and a stable transformation. The mechanical pressure waves are generated by an ultrahigh-pressure short duration pulse incident on a thin aluminum−polydimethylsi-loxane (Al−PDMS) membrane. The pulse is produced through the digital combustion of a nanoengineered composite (comprising of bismuth trioxide (Bi_2O_3) and nanoaluminum (nAl)) packed within a cylindrical chamber (volume ~100 mm^3). The Al−PDMS membrane further transmits the pulse into the column of a fluid that contains the mixture of transforming DNA and cells. The pressure rises to a peak value of 24.3 MPa in the duration of 5.4 μs, as measured by the pressure sensor situated at the bottom of the cuvette containing the biofluid column. We have validated this device design through experimentation related to the transport of GFP plasmid into *E. coli* BL21 transformants. The trans-formation efficiency of the proposed transformation scheme is further compared with the heat shock method[46] and the electroporation method (on the same set of transforming DNA/cells), and the proposed methodology is observed to approach similar efficacy levels as high-voltage electroporation.

■ RESULTS AND DISCUSSION

Theoretical Modeling of Electrical and Pressure Pulse Propagation. We have observed that the maximum trans-formation is achieved with a combination of 40.8 MPa peak pressure (generated by 25 mg Bi_2O_3/nAl)[49] and an electrical signal of 5 V_{pp}. The cell colony counts with varying voltage are listed in Table 1.

It has been observed that at 5 V_{pp} significant cell transformation events take place. Below this voltage, there is no significant transformation. We have further performed a comparison of this new electromechanically coupled process with the heat shock method for bacterial transformation, which is an industry gold standard for transformation processes,[46] and also with electroporation processes. It has been observed that the synchronously acting electromechanical pressure generated in our device is quite efficient in producing transformants higher than the heat shock method, which is almost similar to electroporation processes. The total time for this electromechanical process is around 500 μs, whereas the other standard methods may take several hours.[46] Therefore, the described technique of applying electromechanical shocks is undoubtedly novel and is an effective method to produce rapid transformations within microorganisms.

Figure 2b shows a pressure rise at the bottom of the cuvette, which reaches to 24.3 MPa, as sensed by the pressure sensor. The pressure−time characteristics also indicate an exponential blast pressure−time response containing a sharp pressure rise followed by a decay in the pressure at a slow pace. This specific pressure−time behavior ensures the quick pressurization and a delayed depressurization of the chamber, which gives enough response time to the electric field (just after the half-maxima point). So in the following section, theoretical modeling is carried out to analyze the impact of the electromechanical wave on the mixture of bacterial cells and plasmid. The Al−PDMS membrane can be envisaged to behave like a fixed elastic membrane, positioned normally to the pressure wave (with the Al foil facing the blast side and PDMS facing the biofluidic column side) and is approximated to expand similarly as a freestanding plate.[51] The exponential blast effect on the membrane is approximated by[52]

$$p_i(t) = p_m \, e^{-t/t_{dt}}$$ (1)

where p_i is the incident pressure at any time t, p_m is the maximum incident blast over pressure, and t_{dt} is the wave decay period, which we have approximated to be equal to full width half-maxima time (t_{fwhm}) of normalized pressure−time response. Shock wave density ρ_s and shock wave velocity U_s that reach the assembly are estimated by the Rankine−Hugoniot relation.[51,52]

$$\rho_s = \rho_a \frac{(\gamma + 1)p_m + 2\gamma p_a}{(\gamma - 1)p_m + 2\gamma p_a}$$ (2)

$$U_s = \sqrt{\frac{\gamma p_a}{\rho_a}\left(\frac{(\gamma + 1)p_m}{2\gamma p_a} + 1\right)}$$ (3)

In the above equations, ρ_a is the density of air, p_a is the atmospheric pressure, and γ is the specific heat ratio for air blast. From eqs 2 and 3, the theoretical shock wave velocity is calculated as 6331.124 m/s.

Below this shock wave, the Al−PDMS assembly is situated in a manner so that it transfers the shock wave to the biofluidic column with velocity v_m and through this shock wave, the fluid gets an initial (at time $t = 0$ s) momentum with velocity v_m, membrane velocity. We have further assumed that the biofluidic media is water like, with a very small change in density and sonic velocity even after getting loaded with plasmids.

The total pressure transmitted through the Al−PDMS assembly is calculated through the transmittance coefficient for different interfaces: first, the air−Al interface; second, the Al−PDMS interface, and the third being the PDMS−water (biofluidic medium) interface. The transmittance coefficient T_p is given by[53]

$$T_p = \frac{2Z_2}{Z_1 + Z_2}$$ (4)

where Z (acoustic impedance) = ρc, ρ is the medium density, and c is the velocity of sound in that medium. Considering the properties[53] as mentioned in the Supporting Information (Table S1) of different mediums, the transmittance coefficient has been calculated.

From eqs 1 and 4, the total maximum theoretical pressure at PDMS-biofluidic medium is calculated as 22.11 MPa

(calculations are detailed in the Supporting Information), which is the approximate solution to what we have sensed using a pressure sensor. Further, on the basis of acoustic approximation, the water particle velocity can be theoretically estimated according to Deshpande et al.[52] as

$$v = \frac{p}{c_l \rho_l}$$ (5)

Through this formula, membrane velocity v_m after traveling through the Al−PDMS assembly is found to be 14.1 m/s (c_l is the sound velocity in biofluid and ρ_l is the biofluid density). The expression of motion of the membrane is developed by modifying the equation of striker formulated by Deshpande et al.[52]

$$m\dot{v} = -p = -vc_l\rho_l$$ (6)

In this equation, m is the mass per unit area of the striker ($m = \rho_m \times t_m$) and ρ_m and t_m are the density and thickness of the striker, respectively. In the present study, as the striker constitutes the Al−PDMS assembly, the total mass per unit area is combined. Solving the equation by putting the initial boundary condition, at $t = 0$ and $v = v_m$, the pressure $p(t)$ at $x = 0$ can be expressed as

$$p = v_m c_l \rho_l \exp\left(-\frac{t}{m/(c_l\rho_l)}\right)$$ (7)

For the condition that fluid particles are moving at a constant velocity c_l, the pressure at position x, where x is the length of the column ($x = 8$ mm) can be expressed as

$$p(x, t) = \begin{cases} v_m c_l \rho_l \exp\left(-\dfrac{t - \frac{x}{c_l}}{m/(c_l\rho_l)}\right) & t \geq \dfrac{x}{c_l} \\ 0 & \text{otherwise} \end{cases}$$ (8)

The maximum pressure should be sensed at time $t = 0$ s (in eq 8), but as our pressure sensor is mounted on the other end of the fluid column, we get the maximum pressure as 24.3 MPa (which is nearly similar to the theoretical value) sensed by the pressure sensor from the bottom after a time delay of $t = 5.4$ μs.

From the above theoretical modeling, it can be observed that the pressure generated through the pressurized mechanical pulse is much greater than the elastic modulus of E. coli cells, which is 3 MPa[54] in wet conditions. Hence, the transformation occurs easily as the pressure pulse is applied. As a significant 200 MPa pressure with multiple passes is required to make the E. coli bacteria completely dead,[55] our system works in a permissible range avoiding complete cell lysis. For the electric pulse-assisted case, as the plasmid mixed bacterial cells undergo a high pressure initially through a blast, the requirement of the higher electric field, to the level of electroporation processes may not be needed (the applied electric field between electrodes ≥ 6.25 kV/cm) for transforming E. coli.[24] As per the theoretical formulation, electric field requirement for transformation to occur is given by the Laplace equation

$$U = 1.5rE \cos \theta$$ (9)

where U is the transmembrane voltage, r is the cell radius, and θ is the angle between the static external electric field (E) and site of the membrane where the potential U is measured.[56] At

the poles ($\theta = 0, \pi$), 75% of the voltage drop occurs in the membrane and hence the amplification factor, E_m/E (E_m is a transmembrane electric field) is given by $E_m/E = 1.5r/h$ (h is the cell membrane thickness), which comes out to be 600 for *E. coli* (where $r \approx 2 \mu m$ and $h \approx 5$ nm[57]). In the present study, an optimized low voltage of 5 V (applied electric field between electrodes, $E = 20$ kV/m) is used, which has caused significant gene transformation. This applied field has generated an approximate $E_m = 12\,000$ kV/m ($U_{max\ (at\ \theta=0,\ \pi)} = 60$ mV), which attains efficient gene transformation when the bacteria is held in a 100 mM $CaCl_2$ solution with a high initial blast pressure. All experiments have been carried out in the cuvette maintained at 0 °C. Hence, the transformation is achieved with a voltage, that is ≈ 31 times less than the reported ones.

Due to the application of the synchronized pressure and electric pulses, the period during which the pressure in the system remains above the elastic limit of *E. coli* cells increases and simultaneously transformation levels also increase. Hence, the pressure generated via combining mechanical shock and an electrical field is highly efficacious for the bacterial transformation process.

Although the mechanical pressure is enough to open the pores of the membrane, the generated flux is primarily a diffusional flux. So mainly it is the passive mode of transport of the transforming DNA that is responsible for the transformation. When an additional electric field is applied, there is electrophoretic transport that results in an overall mobility increase. Thus, it can be seen that even at a low electric field of 20 kV/m, enough payload delivery gets initiated and a vast majority of the transforming DNA can enter the cells.

Transformation of *E. coli* BL21. The coupling of the mechanical pressure wave with the electric field-induced pressure is used for transformation of *E. coli* BL21 (a gram-negative bacteria) with GFP-based transforming DNA. We have not conducted any studies through Gram-positive bacteria as that will require separate optimization of pressure/electric pulse combination for transformation. Figure 1 represents a schematic (a) and an actual picture (b) of the fabricated device.

A small amount of Bi_2O_3/nAl nanoenergetic composite (25 mg) is packed inside the combustion chamber (~ 100 mm^3 volume) of the device where a nichrome wire element is digitally triggered to cause microignition of the confined charge inside this device. Among the pressure−time characteristics of various nanoenergetic systems, such as CuO nanorods/Al,[47] Co_3O_4 nanobelts/Al,[48] and Bi_2O_3 nanosquare tablets/Al[49] the Bi_2O_3 nanosquare tablets/Al nanoenergetic material possesses the highest pressurization rates. We have earlier evaluated the pressure−time characteristics of bulk nanoenergetic material using commercially available Bi_2O_3 and Al nanoparticles by igniting 30 mg of this mixture in a pressure cell (Figure 2a).[47,48] The pressure−time characteristic of the Bi_2O_3/nAl nanoenergetic composite, as sensed by the pressure sensor situated at the bottom of the cuvette, is shown in Figure 2b.

When the Bi_2O_3/nAl nanoenergetic composite packed inside the ignition chamber is digitally triggered, a high magnitude of pressure is released. This pressure wave is guided to be incident to Al−PDMS assembled membrane which partitions the ignition chamber from the fluid column present in the cuvettelike portion of the device. The Al−PDMS layer also prevents cross-contamination between the fluid and the nanoenergetic pellets by blocking the reaction products from
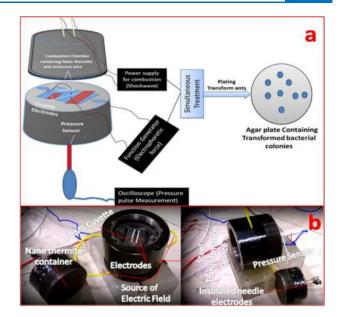

Figure 1. (a) Overall schematic of subsequent events of bacterial gene transformation. (b) Fabricated setup used for bacterial gene transformation.
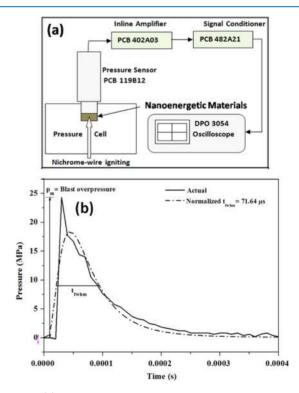

Figure 2. (a) Pressure−time characteristic measurement setup. (b) Pressure−time characteristics of Bi_2O_3/nAl nanoenergetics experienced by the fluid.

falling into the biofluid column. The mechanical pressure wave generated inside the device cavity incident to the Al−PDMS layer transfers the pressure wave to the fluid column, where the sudden hammering of the Al−PDMS membrane with an impact at a high blast pressure increases the local pressure of the fluid almost instantaneously. The pressure rise within this fluid column is measured by placing a pressure sensor at the end opposite to the membrane end of this architecture. The maximum pressure is sensed to be around 24.3 MPa with 25

mg of Bi_2O_3/nAl (Figure 2b) nanoenergetic composite during the transformation procedure. The electric signal is initiated at a delay of ≈85 μs toward the end of the full width half-maxima point of the pressure signal electronically through an in-house developed timing circuit (Figure S1).

We have thoroughly mixed DNA and *E. coli* cells before the application of electric and pressure pulses. Then, the mixture is kept in the cuvette of the device to carry out the transformation. Here, we hypothesize that the electric field pulse leads to the anchoring of the plasmid across the cell membrane and the plasmid is then slowly translocated through the membrane into the cytoplasm. As described earlier, the plasmid is affected by simultaneous treatment of the mechanical and the electrical pressure waves. It is a very well-known phenomenon that when a cell is treated with an electric field, the area of the cell membrane that faces the electrodes gets affected more.[44] According to our hypothesis, the DNA adheres to the cell membrane and makes a strong interaction with the membrane after the application of the electric pulse. We have observed that the maximum cell viability and the most significant number of transformations occur at a DC pulse width of 500 μs. The solution volume that has been used in our studies is around 100 μL, and the chamber has been designed in a manner so that it can provide a homogenous electric field to the mixture of cells and plasmid. In the case the field applied is nonhomogenous, there may be a possibility of dielectrophoresis and cells sticking to the surface. Researchers have shown earlier that DNA will observe dielectrophoretic effects at a low signal frequency.[50]

Calculation of the Transformation Efficiency. The transformation efficiency of the process is observed by standardized plating and culture method over ampicillin-Luria Bertani (LB) agar plates. Hundred microliters of the transformed cell solution is plated on the LB_{amp} plate for counting purpose. The full-grown plates are visualized under a UV transilluminator, and the images are captured through the camera. The colony counting process is automated by importing high-resolution JPEG files of the full-grown plates into ImageJ (Courtesy: NIH) software and performing a particle count on the number of colonies. Figure 3 shows the number of transformed cells through different transformation schemes (i.e., heat shock method, pressure pulse-assisted method, electric pulse-assisted method, combined electrical and pressure pulse-assisted method, and electroporation). Electric pulse-assisted (5 V) and pressure pulse-assisted (24.3 MPa pressure pulse) transformations present transformation at the individual pulse condition of the synchronized pulse.

Through these cell counts, cell transformation efficiency (in CFU/μg) of the individual transformation processes is calculated and represented in Figure 4 (with around a 95% confidence interval). The transformation efficiency of the *E. coli* BL21 as obtained in the current study is in good agreement with the reported literature.[58]

As can be observed from the transformation efficiency plot, the transformation efficiency of the pressurized pulse-assisted transformation ($0.68 \pm 0.034 \times 10^8$ CFU/μg) is almost twice as compared to that of the electric pulse-assisted transformation method ($0.34 \pm 0.017 \times 10^8$ CFU/μg), confirming that the standalone pressure pulse-assisted transformation is more effective than the 5 V electrical pulse-assisted transformation. It can also be observed that these two transformation schemes are quite low in terms of efficiency as compared with the heat shock method ($1.3 \pm 0.065 \times 10^8$
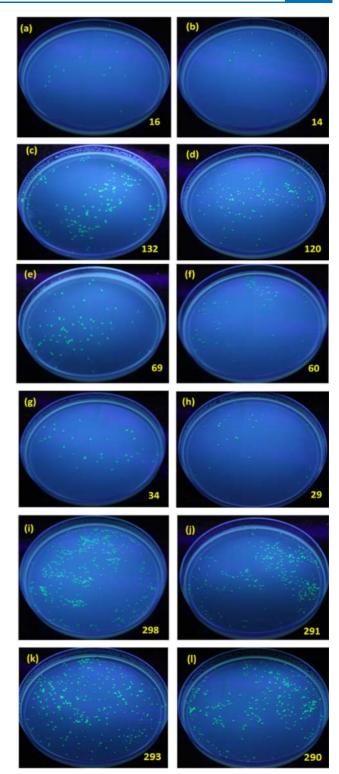

Figure 3. Plating image for colonies of transformants, as visualized under a UV transilluminator (dilution factor = 40, counts reported using ImageJ in colony forming units) for (a, b) control sample 1 and 2; (c, d) Transformed cells via heat shock method: sample 1 and 2; (e, f) transformed cells via mechanically pressurized pulse: sample 1 and 2; (g, h) transformed cells via an electric pulse of 500 μs at 5 VDC: sample 1 and 2; (i, j) transformed cells via coupled mechanical and electrical pressure pulse: sample 1 and 2; (k, l) transformed cells via electroporation.
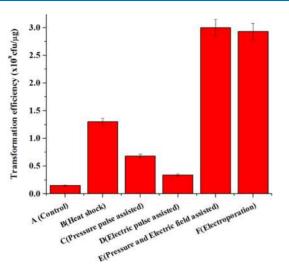
Figure 4. Transformation efficiency related to various transformation schemes (corresponding to three repetitions).

CFU/μg), whereas synchronized pulse (pressure and electric field)-assisted transformation and electroporation are much more efficient than the heat shock method. The transformation efficiency of the synchronized pulse-assisted transformation (the reported transformation scheme) is observed to be $3 \pm 0.15 \times 10^8$ CFU/μg, which is quite similar to the efficacy of the electroporation method ($2.93 \pm 0.14 \times 10^8$ CFU/μg). This confirms that the reported methodology obtains an effective transformation yield, which can be achieved without the need for the very high electric field as used in electroporation, which in turn induces Joule heating and higher cell mortality. The high transformation yield has become possible due to the high-pressure pulse, which opens the pores of the membrane and facilitates the passive transport of DNA that is being further assisted by the smooth electrophoretic transport of this DNA by the use of a low electric field. It can also be observed that as the Joule heating is reduced, the cell mortality is also reduced and the viable cell count is obtained to be higher in the reported method as compared with electroporation (discussed in detail in the next section).

We have also performed confocal imaging of GFP plasmid-transformed *E. coli* cells for further validation of the cell transformation. For carrying out confocal imaging, a single

grown colony is picked from the plated transformed cells and is further grown in LB media. As and when the growth is observed, the cells are washed multiple times with Milli-Q water. Five microliters of cells is dropped on the clean glass slide without any additional staining step and covered with a glass coverslip for confocal imaging. Figure 5 depicts FITC, differential interference contrast (DIC), and combined images of FITC/DIC, which confirms that the *E. coli* cells are transformed with GFP plasmid.

Cell Viability Study. The cell viability is observed to be strongly influenced by the transformation process and is observed by plating 100 μL of the cell solution before and after transformation on an LB agar plate. Figure 6 shows the CFU images of the cell solution before and after the transformation process on the LB plate. Table 2 presents the viable cell count related to different transformation schemes. It can be observed from the transformation scheme that the transformation efficiency of the reported method is almost comparable to that of the electroporation method whereas the viability of the cells through the reported method is better than that of the electroporation. The viability test has shown that the heat shock method shows higher viability as compared with the synchronized pulse-assisted transformation and electroporation.

CONCLUSIONS

The standalone mechanical and pressure waves have not demonstrated sufficient bacterial transformation. However, the bacterial transformation has been observed to be enhanced by the coupling of the mechanical and electrical pressure waves in unison. When an appropriate mechanical pressure pulse in combination with an electric pulse is transmitted to the biological fluid, the transformation yield can be improved significantly. This optimum transformation condition in our case has been obtained by triggering an ignition of 25 mg of the confined nanoenergetic composite and a 5 VDC potential being applied in a time-controlled manner. It can be intuitively understood that the bacterial cells within the fluidic environment experience different magnitudes of mechanical pressure in various areas along the membrane surface mainly as they are oriented differently about the pressure front. Hence, the localized mechanical pressure interacting with the particular bacterial cell should be enough to damage some portions of the cell membrane, which are incident to this pressure wave. From
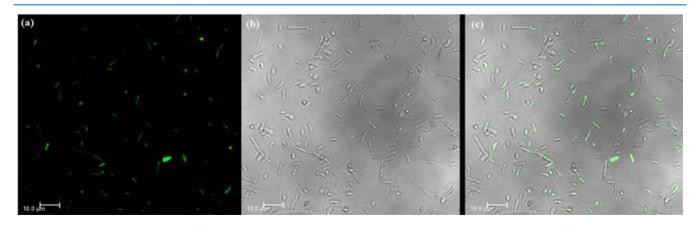

Figure 5. Confocal laser scanning microscopy of transformed *E. coli* cells. (a) FITC image of *E. coli* cells showing GFP expression at 40×. (b) Differential interference contrast (DIC) image of cells under the bright field at 40×. (c) Showing intensity of GFP expression in cells (combined images (a) and (b)).
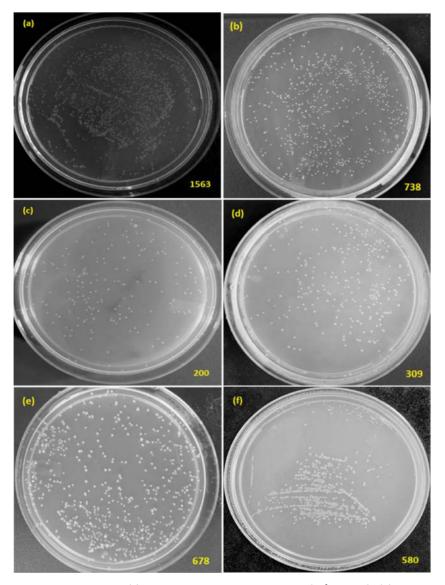
Figure 6. CFU images corresponding to viable cells. (a) Cell solution before transformation (10^5 dilution); (b) viable cells after heat shock method (10^3 dilution); (c) viable cells after mechanically pressurized pulse (10^4 dilution); (d) viable cells after electric pulse of 500 μs at 5 VDC (10^4 dilution); (e) viable cells after synchronized mechanical and electrical pressure pulse (10^3 dilution); (f) viable cells after electroporation (10^3 dilution).

Table 2. Viability Corresponding to Various Transformation Methods

s. no	transformation method	viable cell count (CFU/mL)		percentage of viable cells ($\times 10^{-2}$)
		before transformation	after transformation	
1	heat shock method	1.563×10^9	7.38×10^5	4.72
2	pressure pulse assisted		2×10^6	12.79
3	electric pulse assisted		3.09×10^6	19.76
4	synchronized mechanical and electrical pressure pulse		6.78×10^5	4.33
5	electroporation		5.8×10^5	3.71

a theoretical perspective, it has been observed that the electrical pressure wave helps assist the mechanical pressure on the cellular membrane and also induces electrophoretic transportation of the negatively charged transforming DNA more effectively. The reported methodology has shown a good order of magnitude of the transformation efficiency as compared with the heat shock method or electroporation method.

Additionally, the cell viability that is observed is higher than the electroporation. The overall advantage that we perceive through this process is a definite reduction in time of transformation than other established techniques like heat shock or electroporation. Thus, the reported technology has shown efficacies of transformation similar to other standard methods.

■ EXPERIMENTAL SECTION

Preparation of Nanoenergetic Composites. Nanothermite composites have been prepared by ultrasonic mixing of 200 mg of Bi_2O_3 nanoparticles of average diameter of 90–210 nm (procured from Sigma-Aldrich, India) with 50 mg of Al nanopowder of average diameter of 80 nm (procured from Neo Ecosystem Pvt Ltd India) in isopropyl alcohol (30 mL) in

a Sonics Vibra-Cell ultrasonic processor (model VCX130, 130 W, 20 kHz, Sonics & Materials, Inc.). The ultrasonication process disperses and breaks apart the agglomerates of Bi_2O_3 and Al nanoparticles and promotes homogeneous mixing. The ultrasonication process has been continued for ~10 min in this synthesis by keeping the on−off pulsing time equal to 10 s to avoid any thermal gradient within the solution. Finally, the isopropyl alcohol is evaporated by drying the well-homogenized slurry at 90 °C in a hot air oven and the dried powder is extracted and immediately kept under vacuum to avoid any moisture absorption.

Device Design and Fabrication. The schematic of the synchronous electromechanical pressure generator is shown in Figure 1a, and the actual fabricated device is shown in Figure 1b. The device has been developed by assembling two cylindrical parts fabricated in mild steel.

Realization of the Upper Die. The upper part is a small cylindrical chamber of 100 mm^3 volume containing a pressurized pellet of the nanoenergetic composite. The upper part also consists of two 1 mm diameter holes to hold ignition electrodes to set off the fitted charge as machined by electric discharge machining (EDM). The insulated ignition needle electrodes are plugged with nichrome wires and are connected to an external DC voltage supply through an ON/OFF switch.

Realization of the Lower Die. In the lower part of the device, a rectangular slot (width x length x height: 20 x 27 x 20 cm^3) is machined through EDM for placing the cuvette containing the mixture of cells and GFP plasmid. A through hole of diameter 5 mm perpendicular to the width of the rectangular slot is made for providing external electrical connections to the cuvette electrode. The lower part also carries a slot at the bottom of the device for mounting the pressure sensor (PCB119B12) and a thin cylindrical cavity at the top for housing the separator membrane (Al−PDMS assembly brought together in contact without any air gap).

Reusable and economic PDMS cuvettes have been fabricated through a replication and molding technique, which eventually go into the slot of the cuvette in the lower member for containing the fluid column (a mixture of cells and plasmid). Two Al foils are attached in the middle portion of the replica-molded PDMS (cuvette) for acting as electrodes to generate an electric pulse. The cuvette further comprises of two PDMS layers of different compositions. The one containing a 10:1 ratio (of silicone elastomer and curing agent from Sylgard 184, Dow Corning, Midland) occupies a significant portion of the wall thickness of the cuvette, by the side of the Al electrodes (Figure 1b). It is used for providing strength to the containment of the cuvette, whereas another layer comprising of a 40:1 ratio occupies the bottom portion of the cuvette to allow the transfer of the pressure pulse effectively to the pressure sensor. The central idea behind fabricating this twin layer cuvette is to be able to transfer the pressure wave quickly through the significantly softer layer of PDMS to the pressure sensor that is fitted at the bottom end of the cuvette. The task of the harder layer is to primarily provide a leakage-free containment for the biological fluid in the postblast highly pressurized environment of the chamber. A diffusion/intermixing layer developed in the interface of the two layers eliminates the need for any adhesive joint between the layers.

Assembly of Upper and Lower Dies. The Al (thickness 0.5 mm)-PDMS (thickness 3 mm) membrane separates the cuvette from the nanoenergetic composite and transfers the pressure of the blast to the mixture of cells and plasmid immediately underneath it. This isolating PDMS layer has been prepared using a ratio of 40:1 of silicone elastomer and a curing agent. The upper and lower halves are held to each other by screw threads after putting in place all contents of this device, like nanoenergetic composite pellet, separator membrane, cells, plasmid, etc. The rugged design of this device helps in containing the blast effect sustainably so that the mechanical pressure generated out of the ignition of the nanothermite pellet is focused onto the mixture of cells and plasmid with minimal dissipation.

Pulse Generator Circuit. A pulse generator circuit (shown in Figure S1) is further prepared to feed the electrical signal using an 8 pin 555 IC with variable resistance R and capacitance C, which will delay the timing of the output commensurate with the time needed for the full width half-maxima point of the mechanical pressure pulse. The output (pin number 3) of the IC is connected to the Gate of an IRF 530 metal−oxide−semiconductor field-effect transistor (MOSFET), which is used as a switch for the external voltage applied across the cuvette electrodes. The external voltage is provided by the voltage generator, and its positive terminal is connected to the drain of the MOSFET through a diode and resistance. The electrical output to the cuvette is taken from the Source of the MOSFET and the negative terminal of the external voltage source. The pulsed voltage is varied from 0 to 10 VDC. The whole circuit is operated by a 10 VDC battery. We have performed simulations of the planned circuit through LTSPICE before actual fabrication of the circuitry.

Pressure Measurement. The magnitude of the pressure pulse is sensed at the bottom of the cuvette containing the mixture of cells and plasmid using a pressure sensor (PCB119B12) inserted at the lower end of the cuvette with its sensing wires coming out of the device. The leads of this sensor are attached to an oscilloscope, and the pressure transmitted by the liquid column is recorded with the digital oscilloscope (DPO 3054).

Cells and Plasmid Preparation. *E. coli* BL21 (genotype: F$^-$ *ompT hsd*S$_B$ (r$_B^-$, m$_B^-$) *gal dcm* (DE3)) strain with GFP plasmid has been used for bacterial transformation. The bacterial cells are grown in Luria Bertani (LB) broth at 37 °C. Antibiotic ampicillin (100 μg/mL) has been used for selecting the transformed cells. The cells used in the experiments are freshly prepared competent cells that are grown to a level such that their optical density (OD600) is recorded as ~0.4−0.6. For preparing the chemically competent cells, the grown bacterial cells are washed multiple times with PBS buffer and centrifuged at 4000g for 15 min. The chemically competent cells are finally suspended in 100 mM $CaCl_2$ medium and kept on ice for an hour before use, and then transformation experiments are carried out. For preparing the electrocompetent cells, the grown bacterial cells are washed several times with 10% glycerol and centrifuged at 4000g for 15 min. The electrocompetent cells are finally suspended in 10% glycerol only. GFP plasmid (~4 kb, 40 pg/μL) (SKU: KT60) was purchased from Genei, Bangalore, India. It comprises of a GFP gene (isolated from a bioluminescent jellyfish *Aequorea victoria*) insert cloned into a pUC18 vector under constitutive expression. GFP is mainly chosen for the experiment to increase the visualization of the cells.

Bacterial Transformation Using Electromechanical Pressure Waves. A simple and unique technique to create pressure waves using nanothermite and simultaneous use of a

low-intensity electric field has been developed. One microliter of the purified plasmid is mixed into 100 μL of cells, and this mixture is pipetted inside the cuvette. The pressure waves are produced inside the steel chamber by igniting the nanothermite and simultaneously applying the electric field through the switching circuit as described above. After the experiment, the transformed cells are pipetted out from the cuvette and are directly plated on ampicillin (100 μg/mL)-nutrient agar (LB$_{amp}$) plates at different dilutions. The agar plates are then kept at 37 °C for 18 h. The experiments are confirmed at the end, by observing fluorescence-labeled colonies under the UV transilluminator and processing the collected JPEG images through ImageJ software. The mixture of bacterial cells along with plasmid that is kept at room temperature for the time corresponding to the transformation time of the reported transformation scheme, without any exposure to mechanical/electrical pressure waves, is used as a control sample. Figure 3 represents the images corresponding to two different samples for each transformation condition (control, heat shock method, mechanical pressure pulse assisted, electric pulse assisted, electromechanically pressurized pulse assisted and electroporation). Each experiment is repeated three times with separately grown identical cells and GFP plasmid. Corresponding error bars for the transformation efficiency for all cases have been depicted in Figure 4.

Electroporation has been performed on a MicroPulser Electroporator, Bio-Rad Laboratories, California using Ec1 Mnemonic for *E. coli* (18 kV/cm) with the prepared electrocompetent cells.

■ ASSOCIATED CONTENT

ⓈSupporting Information

The Supporting Information is available free of charge on the ACS Publications website at DOI: 10.1021/acsomega.9b00202.

> Transmitted pressure estimation at the bottom of cuvette, timing circuit diagram (for electric pulse generation) (PDF)

■ AUTHOR INFORMATION

Corresponding Author

*E-mail: bhattacs@iitk.ac.in. Tel: +915122596056. Fax: +91-5122597408.

ORCID ⊙

Shantanu Bhattacharya: 0000-0002-7902-2119

Author Contributions

∥R.K., G.B., and V.K.P. contributed equally to this work.

Author Contributions

R.K. fabricated the pressure generator and associated instrumentation, G.B. performed all gene transformation experiments with R.K., G. B. performed all viability experiments, G.B. and A.G. were involved in developing the computational model for estimating the overall pressure. A.G. was involved in the fabrication of the timing circuit and also contributed to device fabrication. V.K.P. did the synthesis of nanoenergetic materials and D.S. performed all cell culture and GFP expression monitoring with K.M. and M.N., R.K., and G.B. also performed confocal microscopy over transformed cells. S.B., S.G., K.G., and R.G. have jointly provided supervision with necessary planning and ideation for this work. The manuscript has been written by them together with inputs from all other authors. Figure 1a,b is drawn jointly by V.K.P. and A.G. and Figure 2a,b is drawn by V.K.P. and G.B. together. Figures 3−5 are drawn by R.K, D.S., M.N., and G.B. together, Figure 6 is drawn by G. B., and Figure S1 is drawn by R.K.

Notes

The authors declare no competing financial interest.

■ REFERENCES

(1) Loske, A. M.; Campos-Guillen, J.; Fernandez, F.; Castano-Tostado, E. Enhanced Shockwave Assisted Transformation of *Escherichia coli*. *Ultrasound Med. Biol.* **2011**, *37*, 502−510.

(2) Sambrook, J.; Russel, D. *Molecular Cloning: A Laboratory Manual*; Cold spring Harbour: NY, 2001.

(3) Chen, I.; Dubnau, D. DNA Uptake during Bacterial Transformation. *Nat. Rev. Microbiol.* **2004**, *2*, 241−249.

(4) Song, Y.; Hahn, T.; Thompson, I. P.; Mason, T. J.; Preston, G. M.; Li, G.; Paniwnyk, L.; Huang, W. E. Ultrasound-Mediated DNA Transfer for Bacteria. *Nucleic Acids Res.* **2007**, *35*, No. e129.

(5) Garcia-Chaumont, C.; Seksek, O.; Grzybowska, J.; Borowski, E.; Bolard, J. Delivery Systems for Antisense Oligonucleotides. *Pharmacol. Ther.* **2000**, *87*, 255−277.

(6) Mountain, A. Gene Therapy: The First Decade. *Trends Biotechnol.* **2000**, *18*, 119−128.

(7) Waehler, R.; Russell, S. J.; Curiel, D. T. Engineering Targeted Viral Vectors for Gene Therapy. *Nat. Rev. Genet.* **2007**, *8*, 573−587.

(8) Gao, X.; Kim, K. S.; Liu, D. Nonviral Gene Delivery: What We Know And What is Next. *AAPS J.* **2007**, *9*, E92−E104.

(9) Wolf, H.; Rols, M. P.; Boldt, E.; Neumann, E.; Teissie, J. Control by Pulse Parameters of Electric Field-Mediated Gene Transfer in Mammalian Cells. *Biophys. J.* **1994**, *66*, 524−531.

(10) Han, Y. W.; Ikegami, A.; Chung, P.; Zhang, L.; Deng, C. X. Sonoporation is an Efficient Tool for Intracellular Fluorescent Dextran Delivery and One-Step Double-Crossover Mutant Construction in Fusobacterium Nucleatum. *Appl. Environ. Microbiol.* **2007**, *73*, 3677−3683.

(11) Iida, A.; Seki, M.; Kamada, M.; Yamada, Y.; Morikawa, H. Gene Delivery into Cultured Plant Cells by DNA-Coated Gold Particles Accelerated by a Pneumatic Particle Gun. *Theor. Appl. Genet.* **1990**, *80*, 813−816.

(12) Felgner, P. L.; Gadek, T. R.; Holm, M.; Roman, R.; Chan, H. W.; Wenz, M.; Northrop, J. P.; Ringold, G. M.; Danielsen, M. Lipofection: A Highly Efficient, Lipid-Mediated DNA Transfection Procedure. *Proc. Natl. Acad. Sci. U.S.A.* **1987**, *84*, 7413−7417.

(13) Shen, Y. M.; Hirschhorn, R. R.; Mercer, W. E.; Surmacz, E.; Tsutsui, Y.; Soprano, K. J.; Baserga, R. Gene Transfer: DNA Microinjection Compared with DNA Transfection with a Very High Efficiency. *Mol Cell Biol.* **1982**, *2*, 1145−1154.

(14) Huber, P. E.; Pfisterer, P. In Vitro and In Vivo Transfection of Plasmid DNA in the Dunning Prostate Tumor R3327-AT1 is Enhanced by Focused Ultrasound. *Gene Ther.* **2000**, *7*, 1516−1525.

(15) Tiflova, O. A.; Leonov, P. G.; Karbysheva, E. A.; Shakhnabatian, L. G. Effect of He−Ne Laser Irradiation on Plasmid Transformation of *Escherichia coli* Bacteria. *Mikrobiologia* **1997**, *66*, 640−643.

(16) Wilharm, G.; Lepka, D.; Faber, F.; Hofmann, J.; Kerrinnes, T.; Skiebe, E. A Simple and Rapid Method of Bacterial Transformation. *J. Microbiol. Methods* **2010**, *80*, 215−216.

(17) Kodama, T.; Doukas, A. G.; Hamblin, M. R. Shock Wave-Mediated Molecular Delivery into Cells. *Biochim. Biophys. Acta, Mol. Cell Res.* **2002**, *1542*, 186−194.

(18) Gambihler, S.; Delius, M.; Ellwart, J. W. Permeabilization of the Plasma Membrane of L1210 Mouse Leukemia Cells Using Lithotripter Shock Waves. *J. Membr. Biol.* **1994**, *141*, 267−275.

(19) Kodama, T.; Hamblin, M. R.; Doukas, A. G. Cytoplasmic Molecular Delivery with Shock Waves: Importance of Impulse. *Biophys. J.* **2000**, *79*, 1821−1832.

(20) Mulholland, S. E.; Lee, S.; McAuliffe, D. J.; Doukas, A. G. Cell Loading with Laser-Generated Stress Waves: The Role of the Stress Gradient. *Pharm. Res.* **1999**, *16*, 514−518.

(21) Korampally, M.; Apperson, S. J.; Staley, C. S.; Castorena, J. A.; Thiruvengadathan, R.; Gangopadhyay, K.; Mohan, R. R.; Ghosh, A.; Polo-Parada, L.; Gangopadhyay, S. Transient Pressure Mediated Intranuclear Delivery of FITC-Dextran into Chicken Cardiomyocytes by MEMS-Based Nanothermite Reaction Actuator. *Sens. Actuators, B* **2012**, *171−172*, 1292−1296.

(22) Divya Prakash, G.; Anish, R. V.; Jagadeesh, G.; Chakravortty, D. Bacterial Transformation Using Micro-Shock Waves. *Anal. Biochem.* **2011**, *419*, 292−301.

(23) Zimmermann, U.; Pilwat, G.; Friemann, F. Dielectric Breakdown of Cell Membranes. In *Membrane Trans in Plants*; Springer: Berlin, Heidelberg, 1974; pp 146−153.

(24) Taketo, A. DNA Transfection of *Escherichia coli* by Electroporation. *Biochim. Biophys. Acta, Gene Struct. Expression* **1988**, *949*, 318−324.

(25) Weaver, J. C. Electroporation of Cell and Tissues. *IEEE Trans Plasma Sci.* **2000**, *28*, 24−33.

(26) Pliquett, U.; Weaver, J. C. Electroporation of Human Skin: Simultaneous Measurement of Changes in the Transport of Two Florescent Molecules and in the Passive Electrical Properties. *Bioelectrochem. Bioenerg.* **1996**, *39*, 1−12.

(27) Golzio, M.; Teissie, J.; Rols, M. P. Direct Visualization at the Single-Cell Level of Electrically Mediated Gene Delivery. *Proc. Natl. Acad. Sci. U.S.A.* **2002**, *99*, 1292−1297.

(28) Golzio, M.; Rols, M. P.; Teissie, J. In Vitro and In Vivo Electric Field-Mediated Permeabilization, Gene Transfer, and Expression. *Methods* **2004**, *33*, 126−135.

(29) Klenchin, V. A.; Sukharev, S. I.; Serov, S. M.; Chernomordik, L. V.; Yu, A. C. Electrically Induced DNA Uptake by Cells is a Fast Process Involving DNA Electrophoresis. *Biophys. J.* **1991**, *60*, 804−811.

(30) Sukharev, S. I.; Klenchin, V. A.; Serov, S. M.; Chernomordik, L. V.; Yu, A. C. Electroporation and Electrophoretic DNA Transfer into Cells: The Effect of DNA Interaction with Electropores. *Biophys. J.* **1992**, *63*, 1320−1327.

(31) Satkauskas, S.; Bureau, M. F.; Puc, M.; Mahfoudi, A.; Scherman, D.; Miklavcic, D.; Mir, L. M. Mechanisms of In Vivo DNA Electrotransfer: Respective Contributions of Cell Electropermeabilization and DNA Electrophoresis. *Mol. Ther.* **2002**, *5*, 133−140.

(32) MacLachlan, P. R.; Sanderson, K. E. Transformation of *Salmonella typhimurium* with Plasmid DNA: Differences between Rough and Smooth Strains. *J. Bacteriol.* **1985**, *161*, 442−445.

(33) Mercer, A. A.; Loutit, J. S. Transformation and Transfection of *Pseudomonas aeruginosa*: Effects of Metal Ions. *J. Bacteriol.* **1979**, *140*, 37−42.

(34) Neumann, E.; Schaefer-Ridder, M.; Wang, Y.; Hofschneider, P. H. Gene Transfer into Mouse Lyoma Cells by Electroporation in High Electric Fields. *EMBO J.* **1982**, *1*, 841−845.

(35) Aihara, H.; Miyazaki, J. I. Gene Transfer into Muscle by Electroporation In Vivo. *Nat. Biotechnol.* **1998**, *16*, 867−870.

(36) Escoffre, J. M.; Portet, T.; Wasungu, L.; Teissie, J.; Dean, D.; Rols, M. P. What is (Still Not) Known of the Mechanism by Which Electroporation Mediates Gene Transfer and Expression in Cells and Tissues. *Mol. Biotechnol.* **2009**, *41*, 286−295.

(37) Lee, S. W.; Tai, Y. C. A Micro Cell Lysis Device. *Sens. Actuators, A* **1999**, *73*, 74−79.

(38) Huang, Y.; Rubinsky, B. Flow-Through Micro-Electroporation Chip for High Efficiency Single-Cell Genetic Manipulation. *Sens. Actuators, A* **2003**, *104*, 205−212.

(39) Lin, Y. C.; Li, M.; Wu, C. C. Simulation and Experimental Demonstration of the Electric Field Assisted Electroporation Microchip for In Vitro Gene Delivery Enhancement. *Lab Chip* **2004**, *4*, 104−108.

(40) Lu, H.; Schmidt, M. A.; Jensen, K. F. A Microfluidic Electroporation Device for Cell Lysis. *Lab Chip* **2005**, *5*, 23−29.

(41) Khine, M.; Lau, A.; Ionescu-Zanetti, C.; Seo, J.; Lee, L. P. A Single Cell Electroporation Chip. *Lab Chip* **2005**, *5*, 38−43.

(42) Fei, Z.; Wang, S.; Xie, Y.; Henslee, B. E.; Koh, C. G.; Lee, L. J. Gene Transfection of Mammalian Cells Using Membrane Sandwich Electroporation. *Anal. Chem.* **2007**, *79*, 5719−5722.

(43) Ziv, R.; Steinhardt, Y.; Pelled, G.; Gazit, D.; Rubinsky, B. Micro-Electroporation of Mesenchymal Stem Cells with Alternating Electrical Current Pulses. *Biomed. Microdevices* **2009**, *11*, 95−101.

(44) Chang, D. C. Cell Poration and Cell Fusion Using an Oscillating Electric Field. *Biophys. J.* **1989**, *56*, 641−652.

(45) Chang, D. C.; Gao, P. Q.; Maxwell, B. L. High Efficiency Gene Transfection by Electroporation Using a Radio-Frequency Electric Field. *Biochim. Biophys. Acta, Mol. Cell Res.* **1991**, *1092*, 153−160.

(46) Froger, A.; Hall, J. E. Transformation of Plasmid DNA into *E. coli* Using the Heat Shock Method. *J. Visualized Exp.* **2007**, *6*, No. 253.

(47) Patel, V. K.; Bhattacharya, S. High-Performance Nanothermite Composites Based on Aloe-Vera-Assisted CuO Nanorods. *ACS Appl. Mater. Interfaces* **2013**, *5*, 13364−13374.

(48) Patel, V. K.; Saurav, J. R.; Gangopadhyay, K.; Gangopadhyay, S.; Bhattacharya, S. Combustion Characterization and Modeling of Novel Nanoenergetic Composites of Co$_3$O$_4$/nAl. *RSC Adv.* **2015**, *5*, 21471−21479.

(49) Patel, V. K.; Ganguli, A.; Kant, R.; Bhattacharya, S. Micropatterning of Nanoenergetic Films for Pyrotechnics. *RSC Adv.* **2015**, *5*, 14967−14973.

(50) Ying, L.; White, S. S.; Bruckbauer, A.; Meadows, L.; Korchev, Y. E.; Klenerman, D. Frequency and Voltage Dependence of the Dielectrophoretic Trapping of Short Lengths of DNA and dCTP in a Nanopipette. *Biophys. J.* **2004**, *86*, 1018−1027.

(51) Kambouchev, N.; Noels, L.; Radovitzky, R. Fluid Structure Interaction Effects in the Dynamic Response of Free Standing Plates to Uniform Shock Loading. *J Appl. Mech.* **2007**, *74*, 1042−1045.

(52) Deshpande, V. S.; Heaver, A.; Fleck, N. A. (2006) An Underwater Shock Simulator. *Proc. R. Soc. A* **2006**, *462*, 1021−1041.

(53) Rahman, M. F.; Arshad, M. R.; Manaf, A. A.; Yaacob, M. I. An Investigation on the Behavior of PDMS as a Membrane Material for Underwater Acoustic Sensing. *Indian J. Geo-Mar. Sci.* **2012**, *41*, 557−562.

(54) Cerf, A.; Cau, J. C.; Vieu, C.; Dague, E. Nanomechanical Properties of Dead or Alive Single-Patterned Bacteria. *Langmuir* **2009**, *25*, 5731−5736.

(55) Vachon, J. F.; Kheadr, E. E.; Giasson, J.; Paquin, P.; Fliss, I. Inactivation of Foodborne Pathogens in Milk Using Dynamic High Pressure. *J Food Prot.* **2002**, *65*, 345−352.

(56) Weaver, J. C.; Chizmadzhev, Y. A. Theory of Electroporation: A Review. *Bioelectrochem. Bioenerg.* **1996**, *41*, 135−160.

(57) Briegel, A.; Ortega, D. R.; Tocheva, E. I.; Wuichet, K.; Li, Z.; Chen, S.; Muller, A.; Iancu, C. V.; Murphy, G. E.; Dobro, M. J.; Zhulin, I. B.; Jensen, G. J. Universal Architecture of Bacterial Chemoreceptor Arrays. *Proc. Natl. Acad. Sci. U.S.A.* **2009**, *106*, 17181−17186.

(58) Chan, W.; Verma, C. S.; Lane, D. P.; Gan, S. K. A comparison and optimization of methods and factors affecting the transformation of *Escherichia coli. Biosci. Rep.* **2013**, *33*, 931−937.